Journal of ELECTRICAL ENGINEERING, VOL. 52, NO. 1-2, 2001, 3–11

CHATTERING–FREE VARIABLE STRUCTURE CONTROL

Ján Kardoš *

This paper deals with a chattering-free modification of the t-suboptimal position control, *ie* the robustified t-optimal fixed target control. We present an equivalent control approach synthesis whitch satisfies the reaching condition and eliminates the problem of discontinuous control — the high-frequency oscillations. Simulations show both fast and robust resultant overshoot free responses despite the presence of parametric disturbances.

K e y w o r d s: t-suboptimal control, sliding mode, chattering-free, equivalent control, reaching condition

1 INTRODUCTION

T-suboptimal control (TSC) belongs to a class of nonlinear robust control algorithms with driving level commutation. It has been derived using the geometrical approach in position control systems with parameter uncertainty as an application of variable structure systems (VSS) theory to the deterministic t-optimal control (TOC) algorithm [1], [2]. Both TOC and TSC have the property of fast dynamics but in this case, only the latter ensures the transient quality without an overshoot.

Variable structure control uses the sliding mode to trace the serial model of a switching function. Due to parasitic nonlinearities and unmodelled dynamics influence, the sliding mode in real motion control system vanishes and the high-frequency oscillation around the desired trajectory, *ie* chattering, appears [3], [4]. To deal with the chattering phenomenon the boundary layer [5], the saturation nonlinearity [6] or a continuous element of the control algorithm [4] are often introduced. These may, however, result in steady state error and robustness decay. The dither injection, presented in the literature [1], belongs to the special linearisation techniques and gives good results in particular control schemes of discrete nature. A better way of chattering elimination is the reaching law utilisation [7]. Thus, the control in the close vicinity of the switching manifold is similar to the continuous equivalent control, *ie* the mean value of the original VSS control, without any high-frequency oscillations.

In this paper a reaching law application to the t-suboptimal control algorithm is presented. The main contributions of this work are the development and design of a chattering-free t-suboptimal controller and the establishment of conditions under which we can reach the best transient such that the robustness in the presence of parameter uncertainty is achieved.

2 T–SUBOPTIMAL CONTROL

In this chapter we provide a brief summary of the original *t-suboptimal control* [1] without chattering elimination. It has been derived for a single link of a rigid manipulator considering one dominant variable time constant as an influence of the moment of inertia variation.

Let the position control system's plant be described in the error vector space by the phase canonical form

$$\frac{\mathrm{d}\boldsymbol{e}}{\mathrm{d}t} = \left[\dot{e}\,,\, -\frac{1}{T}(Ku + \dot{e})\right]^{\top} \tag{1}$$

where $\boldsymbol{e}$ is the error vector $[e, \dot{e}]^{\top}$, K is for gain, u is the scalar control action input and T is for time constant affected by disturbances. Let the variable parameter T obey

$$T \in \langle T_{\min}, T_{\max}\rangle\,. \tag{2}$$

The goals of the t-suboptimal control have been formulated similarly to those in the t-optimal control framework [2], and are as follows

i) the response should be free of overshoot despite the uncertainty (2),
ii) the dynamics of the closed loop system should be time optimal for at least one value of T from (2) and
iii) the switching function should be linear.

This control strategy can be viewed as a robustification of the t-optimal control. The structure of a t-suboptimal position control system is in Fig. 1 and as can be seen it is identical to the t-optimal one. In this figure, $\boldsymbol{w} = [w, 0]^{\top}$ ($w = \text{cons.}$) represents the closed loop system's reference vector, M is for driving level of the relay element and $\boldsymbol{x}$ is the plant's phase vector. $F(\boldsymbol{e}) \in R$ defines the switching surface and is to be designed.

In accordance with the theory of VSS with driving level commutation, the control law formula

$$u = M\,\mathrm{sgn}(F) \tag{3}$$

* Department of Control and Automation, FEI STU Bratislava, 812 19 Bratislava, Slovakia

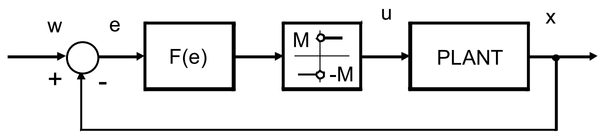

Fig. 1. Principal structure of t-suboptimal position control system

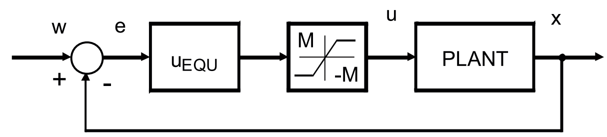

Fig. 2. Equivalent t-suboptimal position control system

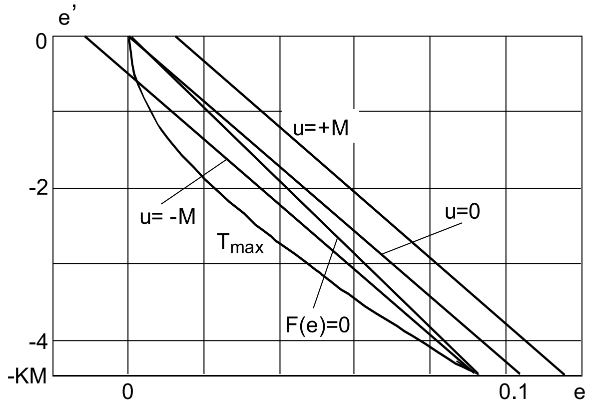

Fig. 3. Phase portrait of the position control system

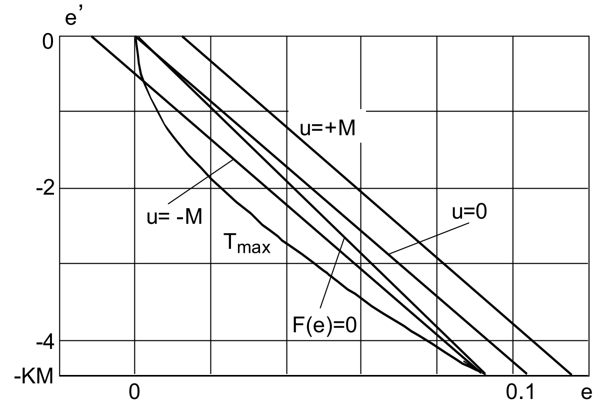

Fig. 4. Control error evolution for $T_{\min}$ and $T_{\max}$ for three types of control algorithm

is discontinuous and therefore the system's behaviour has an oscillating nature. If in the close neighbourhood of the switching manifold the following condition is satisfied

$$F(\boldsymbol{e})\frac{\mathrm{d}F(\boldsymbol{e})}{\mathrm{d}t} < 0 \tag{4}$$

the system is in a *sliding mode* [3] and is insensitive to parameter variations. The condition (4) is known as the sliding mode existence condition or the *reaching condition* for the whole state space [4].

To fulfil the t-suboptimal control goals the geometric approach has been applied. The switching function is expressed as a linear combination of the error vector elements

$$F(\boldsymbol{e})\dot{e} + \alpha e = 0 \tag{5}$$

where α is a positive constant and it is the slope of the switching line (5) in $(e, \dot{e})$ plane. Parameter α is chosen so that for any T from (2) the system's state does not encroach on the region limited by the $\dot{e}$-axis and the worst system's t-optimal rundown (deceleration) trajectory, *ie* the trajectory for $T_{\max}$. To meet this requirement, the switching line should cross the intersection point of the phase portrait asymptote $\dot{e} = \pm KM$ and the above-mentioned trajectory. Thus, the end result of the t-suboptimal control synthesis corresponds to the following α value

$$\alpha = \frac{1}{T_{\max}(1 - \ln 2)}\,. \tag{6}$$

In t-suboptimal control the major part of the system's trajectory (the whole trajectory for both $T = T_{\max}$ and the limit case of $\dot{e} = \pm KE$) is identical to the t-optimal one, the robustness of the sliding mode is exploited only in the final part of the rundown phase.

In conclusion we can say that for the linear switching function (5) gives the solution (6) the best possible system's dynamics for any arbitrary frequency spectra of the parametric disturbance (2) and for arbitrary command w. Moreover, no form of on-line parameter identification should be considered.

3 EQUIVALENT CONTROL

The plant's behaviour in the time domain is described by the set of differential equations (1). To cope with the description of the system's behaviour in the sliding mode where the right-hand side of the system's differential equation is discontinuous (non-analytic), it is inevitable to get the unique solution of the system's trajectory tangential velocity vector, *ie* to perform the so-called regularisation. There were introduced many methods of regularisation but the solutions for a common non-linear system differ, thus the description is not accurate in general. In this chapter we shall prove the uniqueness of the sliding mode description of the controllable canonical form via any regularisation method and give a brief description of the equivalent control approach.

Let the plant be described by the controllable canonical form in the error space

$$\frac{\mathrm{d}\boldsymbol{e}}{\mathrm{d}t} = \left[\dot{e}, \ldots, e^{(n-1)}, f(\boldsymbol{e}, u)\right]^{\top} \tag{7}$$

where $\boldsymbol{e} \in R^n$ stands for the control error vector and f denotes the scalar function (linear or non-linear). Note that the position control system's plant (1) belongs to this category and (7) represents the system's trajectory tangential velocity vector $\boldsymbol{t}$ in the error space.

The sliding mode existence necessary and sufficient condition (4) at point A on the switching surface

$$F(\boldsymbol{e}) = 0 \tag{8}$$

with the control (3) of the plant (7) can be rewritten in the form of the following theorem [1]. Denote $\boldsymbol{n}_A$ the normal vector to the switching surface (8) at A.

THEOREM 1. *Let for one value of control input u be φ_{1A} the convex angle between the normal vector $\boldsymbol{n}_A$ and the tangential velocity vector $\boldsymbol{t}_A$ and similarly be the angle φ_{2A} for the opposite value of u. System (7) will be in the sliding mode at point A on the switching surface (8) if and only if*

$$\operatorname{sgn}\big(\cos(\varphi_{1A})\big) = -\operatorname{sgn}\big(\cos(\varphi_{2A})\big)\,. \tag{9}$$

P r o o f . See reference [1].

Directly from Theorem 1 follows the next lemma.

LEMMA 1. *The controlled plant (7) does not fulfil condition (9) of Theorem 1 on any part of the switching surface (8) which is parallel to the $e^{(n-1)}$ axis of the error space.*

P r o o f . We can get any of values of $\cos(\varphi_A)$ as the normalised inner product of the normal vector $\boldsymbol{n}_A$ and tangential velocity vector $\boldsymbol{t}_A$. These vectors are defined as follows

$$\boldsymbol{n}_A = \Big(\frac{\partial F(\boldsymbol{e})}{\partial \boldsymbol{e}}\Big)_A \tag{10}$$

and

$$\boldsymbol{t}_A = \Big(\frac{\mathrm{d}\boldsymbol{e}}{\mathrm{d}t}\Big)_{A,u}\,. \tag{11}$$

For both opposite values of u, from (7), it is obvious that the only possibility to change the sign of the $\cos(\varphi_A)$ has the nth element of the $\boldsymbol{t}_A$ vector. For the nth element of the normal vector $\boldsymbol{n}_A$ on the switching surface's part parallel to the $e^{(n-1)}$ axis holds

$$\Big(\frac{\partial F(\boldsymbol{e})}{\partial e^{(n-1)}}\Big)_A = 0\,. \tag{12}$$

Therefore the $\cos(\varphi_A)$ can not change the sign and this completes the proof.

Now we are ready to prove the uniqueness of the plant's (7) sliding mode description.

THEOREM 2. *Any of the regularisation methods of the controllable canonical form (7) gives the unique description of the plant's sliding mode behaviour.*

P r o o f . Let $T_A(\boldsymbol{e}) = 0$ denote the tangential hyperplane to the switching surface (8) at point A. Let the system (7) be in the sliding mode at point A, *ie* the system's trajectory traces the switching surface (8) and the plant's velocity vector lies in the tangential hyperplane. The first $(n-1)$ coordinates of the tangential velocity vector are uniquely described by the first $(n-1)$ elements of the system (7), regardless of the regularisation method. According to Lemma 1, for these $(n-1)$ coordinates there exists only one nth coordinate of the plant's velocity vector in the sliding mode, uniquely associated with the hyperplane $T_A(\boldsymbol{e}) = 0$. Thus, there exists only one possible tangential velocity vector describing the system's sliding mode behaviour.

This completes the proof.

The *equivalent control* represents the continuous equivalent of the discontinuous sliding mode control algorithm with identical behaviour, *ie* the equivalent control forces the plant's trajectory to follow the switching surface. The aim is to find the control u_{equ} equivalent to the mean value of the high-frequency control action input u in sliding mode. To keep the system's trajectory on the switching surface (8), the following condition should be satisfied

$$\frac{\mathrm{d}F(\boldsymbol{e})}{\mathrm{d}t}\Big|_{u=u_{equ}} = 0 \tag{13}$$

for the initial condition

$$F\big(\boldsymbol{e}(0)\big) = 0\,. \tag{14}$$

Solving (13) for u, assuming (7), yields the equivalent control u_{equ}, provided that there exists the explicit solution u of

$$\frac{\mathrm{d}e^{(n-1)}}{\mathrm{d}t} = f(\boldsymbol{e}, u)\,. \tag{15}$$

According to (3), u_{equ} satisfies the conditions

$$\min(u) \le u_{equ} \le \max(u)\,. \tag{16}$$

The analytical description of the sliding mode behaviour using the equivalent control approach is summarised in the next theorem.

THEOREM 3. *The sliding mode behaviour of the nth-order system (7) is described by the reduced differential equation (8) of order $(n-1)$ of the switching manifold for the initial condition (14).*

P r o o f . Applying (13) to (7) and (8) gives

$$\frac{\mathrm{d}F(\boldsymbol{e})}{\mathrm{d}t}\Big|_{u=u_{equ}} = \Big(\frac{\partial F(\boldsymbol{e})}{\partial \boldsymbol{e}}\Big)^{\top}\frac{\mathrm{d}\boldsymbol{e}}{\mathrm{d}t}\Big|_{u=u_{equ}} = \frac{\partial F}{\partial e}\frac{\mathrm{d}e}{\mathrm{d}t} + \dots + \frac{\partial F}{\partial e^{(n-2)}}\frac{\mathrm{d}e^{(n-2)}}{\mathrm{d}t} + \frac{\partial F}{\partial e^{(n-1)}} f\big(\boldsymbol{e}, u_{equ}\big) = 0\,. \tag{17}$$

Hence by Lemma 1, without necessity of solving the equation (17) with respect to u_{equ}, substituting (17) to (7), the differential equation of the sliding mode is found

$$\frac{\mathrm{d}e^{(n-1)}}{\mathrm{d}t} = -\frac{1}{\frac{\partial F}{\partial e^{(n-1)}}}\Big(\frac{\partial F}{\partial e}\frac{\mathrm{d}e}{\mathrm{d}t} + \cdots + \frac{\partial F}{\partial e^{(n-2)}}\frac{\mathrm{d}e^{(n-2)}}{\mathrm{d}t}\Big). \tag{18}$$

Integrating the implicit form of equation (18) for the initial condition (14) yields

$$F(\boldsymbol{e}) = 0 \tag{19}$$

which is identical to the switching surface (8) and represents the differential equation of order $(n-1)$ for the control error. This completes the proof.

Theorem 3 gives the solution of the robustness problem via sliding mode control — the system in the sliding mode is described by the switching function differential equation and it is completely insensitive to plant's parametric and external disturbances.

Let us focus our attention on the sliding mode description of the t-suboptimal position control system. Applying (13) to (1) and (5) gives

$$u_{equ} = \frac{1}{K}(\alpha T - 1)\dot{e} \tag{20}$$

which corresponds to the D-regulator output. Control (20) keeps the system's trajectory on the switching surface (8) only if the initial condition

$$\dot{e}(0) = -\alpha e(0) \tag{21}$$

is fulfilled.

According to Theorem 2, the system's trajectory in sliding mode is described by the differential equation

$$\frac{\mathrm{d}e}{\mathrm{d}t} + \alpha e = 0 \tag{22}$$

for the initial condition (21). The solution of (21) and (22) gives the exponential decay of the control error in the time domain

$$e(t) = e(0)\exp(-\alpha t). \tag{23}$$

In general, the steeper is the slope α of the switching line (5) the faster is the transient response in sliding mode.

4 EQUIVALENT T–SUBOPTIMAL CONTROL

The sliding mode control in real systems suffers from a significant drawback — chattering. This stands for the high-frequency oscillation excited by the discontinuous control law (3) due to the presence of parasitic dynamics and nonlinearities. In this chapter we introduce a chattering-free continuous modification of the t-suboptimal control preserving its robustness and dynamism.

We formulate the requirements for the control law as follows:

i) the quality of the control should be comparable to the t-suboptimal one (*cf* goals in chapter 2),

ii) the control should be continuous and chattering-free.

The continuous equivalent control (20) keeps the system's trajectory on the switching surface (8), provided that the plant's parameters are constant and the error vector initial condition satisfies (14). In case of parametric uncertainty (2) and out of the switching manifold (8) the equivalent control algorithm fails. This is the consequence of the fact, that except for the switching surface (8) the equivalent control does not fulfil the condition (4).

Let us define the switching function $F(\boldsymbol{e})$ behaviour by the differential equation

$$\frac{\mathrm{d}F(\boldsymbol{e})}{\mathrm{d}t} = -kF(\boldsymbol{e}) \tag{24}$$

where k is a positive constant.

From (13) and (24) it can be seen that the control guaranteeing the fulfilment of (24) is on the switching surface, *ie* for $F(\boldsymbol{e}) = 0$, identical to the equivalent control. Moreover, according to (24), condition (4) holds for the whole state space. This ensures that at any point of the state space the plant's trajectory tends towards the sliding manifold. In other words, the differential equation (24) represents the *sliding mode reaching condition*. From (24) it is evident that the switching function $F(\boldsymbol{e})$ exponentially decays in the time domain with the time constant $1/k$.

Similarly to t-suboptimal control, let the equivalent control u_{EQU} be the control of plant (1) and (2) satisfying (5), (6) and also the reaching condition (24). Substituting (1) and (5) into (24) yields

$$u_{EQU} = \frac{1}{K}\left[(\alpha T_u - 1)\dot{e} + kT_u(\dot{e} + \alpha e)\right] \tag{25}$$

where $T_u > 0$ denotes for the moment an unknown time constant originating from the plant's parameter uncertainty (2). Note that on the switching surface (5), expression (25), except for T_u, equals to (20) as mentioned earlier. It can be seen from (25) that the continuous control u_{EQU} consists of two typical components — the proportional part with the gain

$$K_P = \frac{\alpha k T_u}{K} \tag{26}$$

and the derivative one with the corresponding gain

$$K_D = \frac{(\alpha + k)T_u - 1}{K}. \tag{27}$$

Now, let us focus our attention on restrictions imposed on the equivalent control parameters T_u and k.

THEOREM 4. *For the equivalent control* (25) *of the system* (1), (2), (5) *and* (6), *the sufficient condition to ensure the non-oscillating character of the transient is*

$$T_u \geq T_{\max}\,. \tag{28}$$

P r o o f . Substituting (25) in (1) gives the second order differential equation of the system's closed-loop dynamics

$$\frac{\mathrm{d}^2 e}{\mathrm{d}t^2} + \frac{T_u}{T}(\alpha + k)\frac{\mathrm{d}e}{\mathrm{d}t} + \frac{T_u}{T}\alpha k e = 0 \tag{29}$$

with damping ratio

$$b = \frac{1}{2}\frac{\alpha + k}{\alpha k}\sqrt{\frac{T_u}{T}\alpha k}\,. \tag{30}$$

For non-oscillating behaviour of the control error e it is necessary to keep the damping ratio b greater or equal to unity, *ie* to fulfil the condition

$$\sqrt{\frac{T_u}{T}}(\alpha + k) \geq 2\sqrt{\alpha k}\,. \tag{31}$$

Note that α and k are positive constants. It is trivial, after some algebra, to prove (31) for $T_u = T$. Evidently, (31) is also valid for all $T_u > T$. According to the above and to parameter uncertainty (2), expression (28) represents the sufficient condition of the non-oscillating behaviour of the dynamics (29). This completes the proof.

In order to meet the requirements set on the desired control, it is necessary to reach the fast development of the switching function (5). This corresponds, according to (24), to the high value of the control parameter k and implies the possible control action constraint in a real system. In agreement with the original TSC, we should limit the value of the new control action to M as follows

$$u_{ETSC} = \begin{cases} u_{EQU} & \text{for abs}(u_{EQU}) < M \\ M\,\mathrm{sgn}(u_{EQU} & \text{for abs}(u_{EQU}) \geq M \end{cases} \tag{32}$$

where u_{ETSC} stands for the proposed *equivalent t-suboptimal control*.

The block diagram of the equivalent t-suboptimal control system is presented in Fig. 2. The difference between this control structure and the original TSC structure is minimal, as seen in Figures 1 and 2. In both structures, the linear part of the control algorithm represents a PD-regulator. As for the non-linear part, a limiter in equivalent t-suboptimal control structure substitutes the relay element in TSC.

The continuous control u_{ETSC} is within the region of the constraint M identical to the original t-suboptimal control. The linear control u_{EQU} is active only in a particular area of the $(e, \dot{e})$ plane in the vicinity of the switching manifold (5). Let us specify the boundaries of this control area. Comparing (25) with $\pm M$ yields

$$\frac{1}{\alpha k T_u}\left[-KM - \big((\alpha + k)T_u - 1\big)\dot{e}\right] \leq e \leq \frac{1}{\alpha k T_u}\left[KM - \big((\alpha + k)T_u - 1\big)\dot{e}\right]\,. \tag{33}$$

The following interpretation of expression (33) is more illustrative. The linear phase u_{EQU} of the equivalent t-suboptimal control is concentrated in a zone of width (in the direction of the e-coordinate)

$$\pm\frac{KM}{\alpha k T_u} \tag{34}$$

around the line of the zero control action

$$\dot{e} = -\frac{\alpha k T_u}{(\alpha + k)T_u - 1}e\,. \tag{35}$$

The relevant parts of the system's phase portrait are given in Fig. 3. In this figure, line (35) is labelled $u = 0$ and similarly are the boundaries $u = M$ and $u = -M$. $F(\boldsymbol{e}) = 0$ denotes the original t-suboptimal switching line (5). Trajectory marked $T_{\max}$ is one of the plant's t-optimal rundown trajectories.

Although line (35) seems to play a role of a new switching line, it should be emphasised that the fulfilment of the reaching condition (24) with respect to the switching line (5) is ensured at any time instant of the transient within the linearity zone (34), (35). As can be seen from (34) and (35), to keep the line (35) close to the switching line (5), *ie* to reach the convergence of both the equivalent t-suboptimal control and the TSC dynamics, it is important to satisfy the condition

$$k \gg 1 \tag{36}$$

which corresponds to the requirement of the fast switching function dynamics (24).

Condition (36) ensures both the width (34) of the linearity zone reduction and the coincidence of the slope of line (35) with the parameter α of the switching line (5), particularly if the condition

$$k \gg \alpha \tag{37}$$

is fulfilled.

As can be seen from (32), the reaching condition (24) is not explicitly fulfilled out of the linearity zone (34) and (35). The system's trajectory can leave this zone, provided that the variable parameter T exceeds the critical value T_{crit} corresponding to the sliding mode decay. Despite this fact we can prove that the system's (1) trajectory returns to the switching manifold (5). Joining expressions (1), (5) and (9) we obtain

$$T_{\mathrm{crit}} = \frac{2}{\alpha}\,. \tag{38}$$

For the control action $u = \pm M$, the switching function evolution contains a global extreme. Setting the first

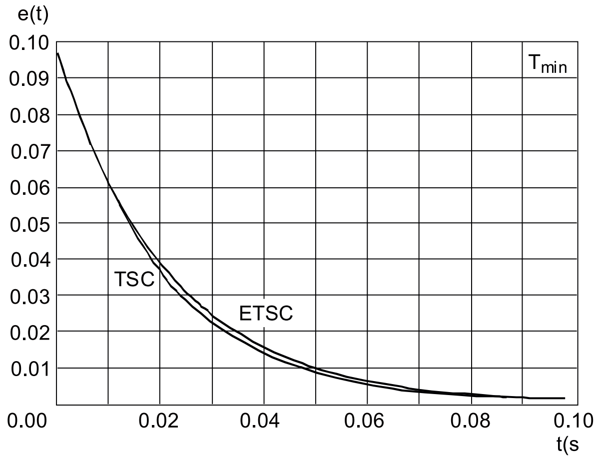

Fig. 5. Rundown phase of control error for TSC and ETSC and for $T_{\min}$

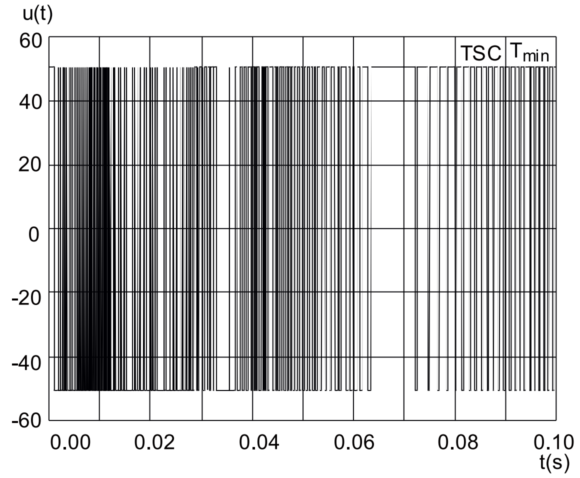

Fig. 6. Control action chattering for TSC and $T_{\min}$

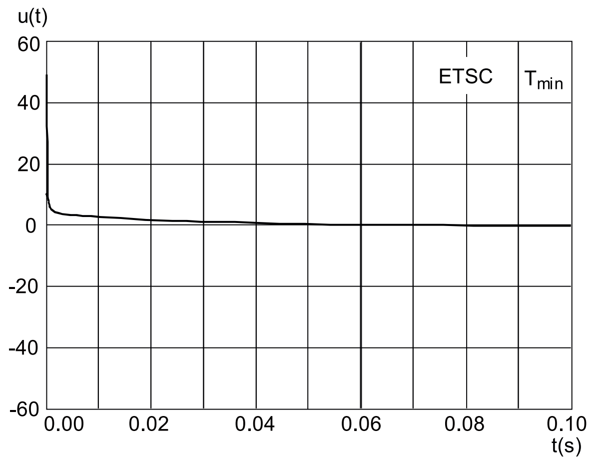

Fig. 7. Control action plot for ETSC and $T_{\min}$

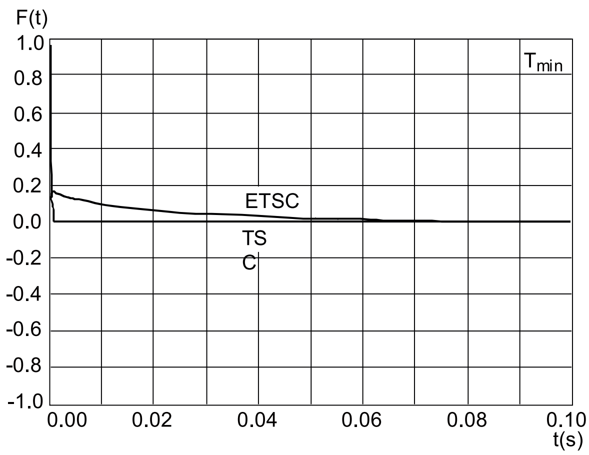

Fig. 8. Switching function evolution for TSC and ETSC and for $T_{\min}$

derivative of (5) equal to zero gives the $\dot{e}$ coordinate of this extreme

$$\dot{e} = \frac{Ku}{\alpha T - 1}\,. \tag{39}$$

Substituting (39) to the second derivative of (5) yields

$$\frac{\mathrm{d}^2 F}{\mathrm{d}t^2} = -\frac{\alpha K u}{T}\,. \tag{40}$$

According to (40), the switching function reaches for $u = -M$ its global minimum (or for $u = M$ the global maximum) and then returns to the zero value, *ie* the system's trajectory returns to the switching manifold.

Note that condition (28) in Theorem 4 prevents any doubt about an overshoot of the plant's (1) response in the presented control. From the phase portrait in Fig. 3, it can be seen that to solve the problem of the possible overshoot, the switching line (5) should be steeper than line (35). Comparing (6) and (35) yields

$$T_u > (1 - \ln 2) T_{\max}\,. \tag{41}$$

Similarly, the intersection point of the phase portrait asymptote $\dot{e} = -KM$ with the switching line (5) should be closer to the $\dot{e}$-axis than the one with the line (35). Comparing the e-coordinates of these two points (*cf* (5), (6) and (35)) yields

$$T_u > 2(1 - \ln 2) T_{\max}\,. \tag{42}$$

Theorem 4 meets both of the last conditions.

The properties of the equivalent t-suboptimal control can be summarised as follows. The control algorithm is described by expressions (25) and (32) with parameter values (6), (28), (36) and (37). We expect that despite the parameter uncertainty (2) the response will be both chattering and overshoot free with the dynamics close to the t-optimal one. Note that only the boundary values of the disturbance (2), without the time behaviour of the variable parameter, are assumed to be known.

5 SIMULATION RESULTS

The proposed equivalent t-suboptimal control algorithm has been applied to a position control model

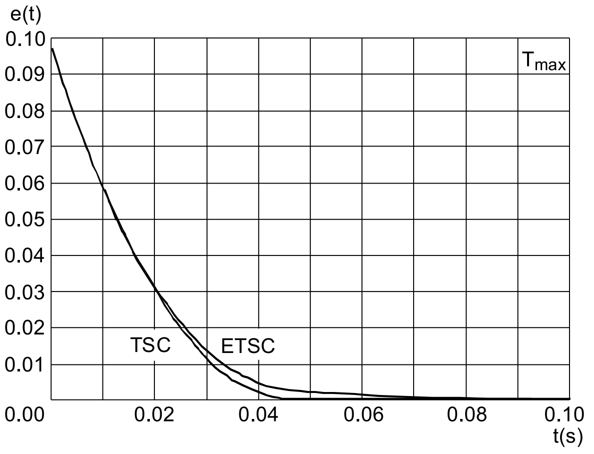

Fig. 9. Rundown phase of control error for TSC and ETSC and for $T_{\max}$

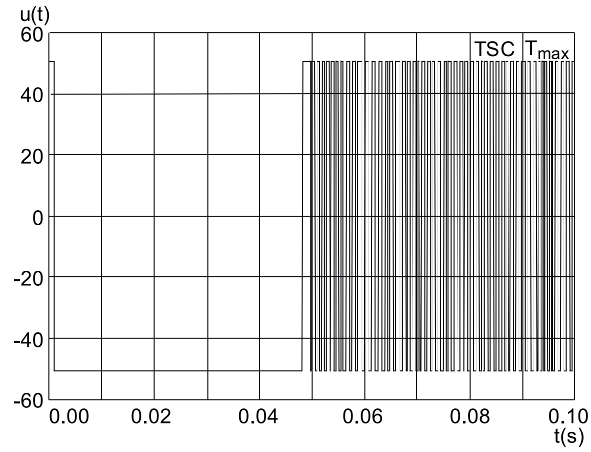

Fig. 10. Control action chattering for TSC and $T_{\max}$

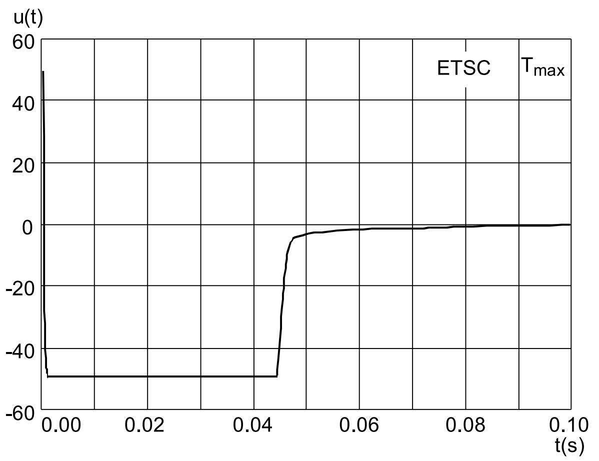

Fig. 11. Control action plot for ETSC and $T_{\max}$

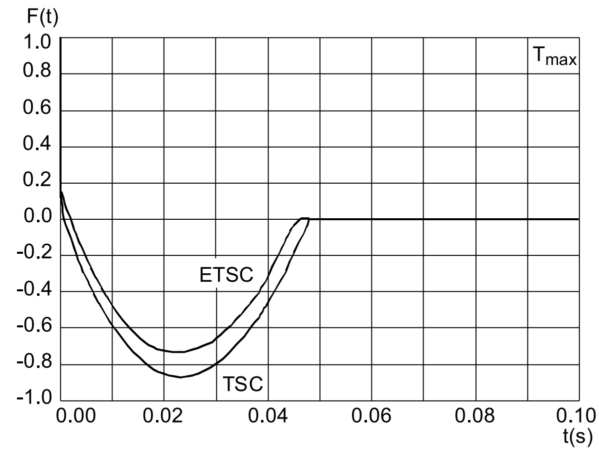

Fig. 12. Switching function evolution for TSC and ETSC and for $T_{\max}$

(1) with parameters corresponding to a real electromechanical chain (PWM converter — DC motor — harmonic drive HD — incremental position/velocity sensor). The parametric disturbance represents the variation of the reduced moment of inertia at the motor shaft. The values of parameters have been as follows: the chain total gain $K = 0.0883$, the boundaries of parametric uncertainty (2) $T_{\min} = 0.018$ s and $T_{\max} = 0.068$ s. The reference input $w = 0.2$ is equivalent to the HD's output shaft angle position 51°. To fulfil conditions (28), (36) and (37), the control parameters were chosen as follows

$$T_u = T_{\max} \qquad \text{and} \qquad k = 1000 \tag{43}$$

which represents the α to k ratio $1:20$.

To simulate the influence of parasitic dynamics presence, the ratio of its equivalent time constant T_P to plant's time constant $T_{\max}$ was chosen also $1:20$.

Note that we should focus our attention on the rundown phase of the transient because this is the only phase where the equivalent t-suboptimal control differs from TSC. Moreover, the main part of the control process, particularly the start-up (acceleration) phase, is identical to that of the t-optimal one, as mentioned earlier. Only Fig. 4 illustrates the whole transient in time domain. In this figure, three control algorithms for both boundary values $T_{\min}$ and $T_{\max}$ of the parametric uncertainty are compared: TOC is for t-optimal control, TSC for t-suboptimal control and ETSC for equivalent t-suboptimal one. The plots show the high quality of the ETSC process — no overshoot and fast dynamics close to TOC. It can be seen that at this resolution all three responses for $T_{\max}$ value coincide. For time constant $T_{\min}$ only TOC slightly differs. The short delay of TSC and ETSC is the price paid for the system robustness in sliding mode. This figure shows the fulfilment of both the t-suboptimal control goals (chapter 2) and the requirement i) for the equivalent t-suboptimal control law (chapter 4).

Following pictures show only the detailed plots within the time interval of the rundown phase.

The first group of figures (see figures 5–8) depicts the responses for $T = T_{\min}$ with the whole rundown phase in sliding mode (*cf* sliding mode existence condition (4)). The control error plot in Fig. 5 has an exponential character due to the linear switching function (5). As a result of the high value of parameter k, the linearity zone (34) is

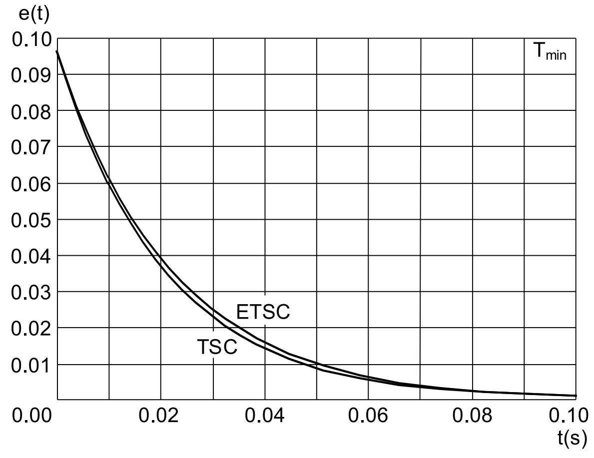

Fig. 13. Rundown phase of control error for TSC and ETSC and for $T_{\min}$ in the presence of parasitic dynamics

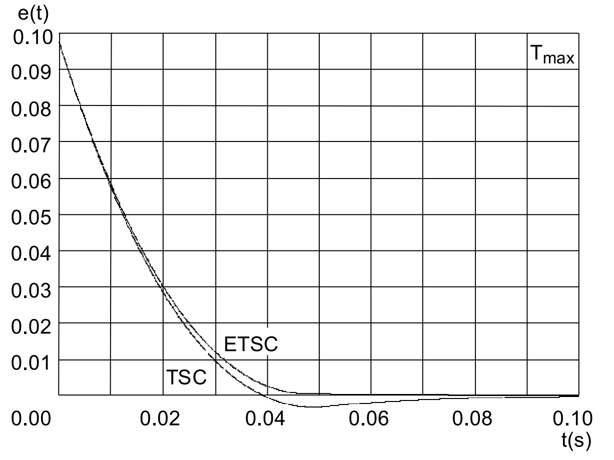

Fig. 14. Rundown phase of control error for TSC and ETSC and for $T_{\max}$ in the presence of parasitic dynamics

very narrow and the difference between ETSC and TSC is minimal.

The resulting plots of the control action chattering for TSC and the smooth evolution of u for ETSC are given in Figs. 6 and 7 respectively. These figures clearly show the advantage of the chattering-free equivalent t-suboptimal algorithm (32) over the discontinuous TSC (3). Note that according to (13) and (24), the u_{ETSC} plot may be viewed as a mean value of the u_{TSC} chattering.

To prove this statement, the evolution of the switching function during the rundown period has been depicted (see Fig. 8). Both the values of the switching function (5) for TSC and ETSC are close to zero. Thus, the u_{ETSC} plot represents the approximate solution of (24) on the switching surface (8) for the initial condition (14), *ie* the equivalent control u_{equ} (20). From Fig. 8, it can be seen the monotonous exponential decay of the switching function evolution for ETSC in agreement with the differential equation (24) within the linearity zone (34).

Similarly to the first group of figures, the second group (see figures 9–12) depicts the responses for the time constant $T = T_{\max}$. According to t-suboptimal control goals (chapter 2), in this case is the system's trajectory for TSC identical to the t-optimal one and the sliding in rundown phase is not present. Figure 9 shows the control error plot of both the TSC and ETSC transients. Evidently, no response can be faster than that of TSC. The short delay of the ETSC control error occurs due to the linearity zone (34). Nevertheless, the dynamics of the equivalent t-suboptimal control is comparable to the t-suboptimal one.

Figures 10 and 11 show the control action behaviour for TSC and ETSC respectively. It can be seen that in the rundown period neither TSC nor ETSC suffers from a chattering. This appears only in the steady state of the t-suboptimal control (see Fig. 10). There is again no doubt about the quality of the proposed equivalent t-suboptimal control (Fig. 11). The control action plot proves the time optimal behaviour of the ETSC transient, except for the narrow linearity zone (34).

According to the t-optimality of the main part of the ETSC transient, the switching function evolution is very similar to the TSC one, as can be seen in Fig. 12. The time constant $T_{\max}$ is greater than the critical value T_{crit} (38). The consequence is that the switching function curve contains a global minimum, as mentioned in chapter 4 (see (39) and (40)). Only in the close vicinity of the zero value — within the linearity zone (34) and (35) — is the switching function behaviour of ETSC described by the reaching condition (24), the rest of the plot corresponds to the t-optimal behaviour.

The robustness of the t-suboptimal type algorithms against the parasitic dynamics presence in a real plant can be seen in Fig. 13 and 14 for $T_{\min}$ and $T_{\max}$ respectively. It should be reminded that the ratio of parasitic dynamics equivalent time constant T_P to plant's time constant $T_{\max}$ equals to $1 : 20$. Comparing Fig. 13 with Fig. 5 we see that for $T = T_{\min}$ there is no difference between the quality for both TSC and ETSC with or without the parasitic dynamics presence. On the other hand, Fig. 14 with $T = T_{\max}$ clearly demonstrates the advantage of the ETSC law over the TSC one. The parasitic dynamics presence results in an overshoot of the error response in TSC but no in ETSC. As for the response time, it is practically identical to that in Fig. 9.

It can be concluded that the proposed equivalent t-suboptimal control meets the requirement of robustness against the parametric disturbance (2) preserving the fast dynamics without both the overshoot and chattering despite the parasitic dynamics presence, as formulated in chapter 4.

6 CONCLUSION

In this paper a chattering-free modification of t-suboptimal control has been proposed including a brief summary of the original TSC theory and the equivalent control approach. The uniqueness of the sliding mode description for the controllable canonical form has been formulated and proved in two theorems. The discontinuous sliding mode typical for variable structure systems has been replaced by a smooth equivalent control algorithm satisfying the reaching condition. After a thorough discussion, the conditions for the control parameters have been determined. The efficiency of the proposed approach has been demonstrated through numerical simulation of a position control system. It has been shown that the control law is robust against parameter variations and parasitic dynamics presence. The results showed ideal control action behaviour and consequently offered a low energy consumption in comparison with the t-suboptimal control law results.

References

[1] KARDOŠ, J.: Variable Structure Motion Control Systems, In B. Frankovi, editor, Trends in Control Theory and Applications, Bratislava, Veda Publishing House, 1999, 132–158.

[2] KARDOŠ, J.—KALAŠ, D.: Near-to-minimum Time VSS with Application to Position Control, Journal of Electrical Engineering **45** No. 12 (1994), 441–452.

[3] UTKIN, V. I.: Sliding Modes and their Applications in Variable Structure Systems, Mir Publishers, Moscow, 1978.

[4] HUNG, J. Y.—GAO, W.—HUNG, J. C.: Variable Structure Control: A Survey, IEEE Trans. on Industrial Electronics **40** No. 1 (1993), 2–22.

[5] KACHROO, P.: Existence of Solutions to a Class of Nonlinear Convergent Chattering-free Sliding Mode Control Systems, IEEE Trans. on Automatic Control **44** No. 8 (1999), 1620–1624.

[6] MOALLEM, M.—KHORASANI, K.—PATEL, R. V.: Inversion-based Sliding Control of a Flexible-link Manipulator, International Journal of Control **71** No. 3 (1998), 477–490.

[7] BARTOSZEWICZ, A.: Discrete-Time Quasi-Sliding-Mode Control Strategies, IEEE Transactions on Industrial Electronics **45** No. 4 (1998), 633–637.

Received 13 July 2000

Ján Kardoš (Ing), received the MS in electrical engineering from the Faculty of Electrical Engineering of the Slovak University of Technoloy in Bratislava, in 1976. Currently he is a senior lecturer at the Department of Control andAutomation of the Faculty of Electrical Engineering of the Slovak University of Technoloy in Bratislava. His main field of interest is motion control and robotics.